Modeled Impact of Anthropogenic Land Cover Change on Climate

KIRSTEN L. FINDELL
NOAA/Geophysical Fluid Dynamics Laboratory, Princeton, New Jersey

ELENA SHEVLIAKOVA
Department of Ecology and Evolutionary Biology, Princeton University, Princeton, New Jersey

P. C. D. MILLY
U.S. Geological Survey, Princeton, New Jersey

RONALD J. STOUFFER
NOAA/Geophysical Fluid Dynamics Laboratory, Princeton, New Jersey

(Manuscript received 18 April 2006, in final form 25 October 2006)

ABSTRACT

Equilibrium experiments with the Geophysical Fluid Dynamics Laboratory's climate model are used to investigate the impact of anthropogenic land cover change on climate. Regions of altered land cover include large portions of Europe, India, eastern China, and the eastern United States. Smaller areas of change are present in various tropical regions. This study focuses on the impacts of biophysical changes associated with the land cover change (albedo, root and stomatal properties, roughness length), which is almost exclusively a conversion from forest to grassland in the model; the effects of irrigation or other water management practices and the effects of atmospheric carbon dioxide changes associated with land cover conversion are not included in these experiments.

The model suggests that observed land cover changes have little or no impact on globally averaged climatic variables (e.g., 2-m air temperature is 0.008 K warmer in a simulation with 1990 land cover compared to a simulation with potential natural vegetation cover). Differences in the annual mean climatic fields analyzed did not exhibit global field significance. Within some of the regions of land cover change, however, there are relatively large changes of many surface climatic variables. These changes are highly significant locally in the annual mean and in most months of the year in eastern Europe and northern India. They can be explained mainly as direct and indirect consequences of model-prescribed increases in surface albedo, decreases in rooting depth, and changes of stomatal control that accompany deforestation.

1. Introduction

Climate models are increasing in complexity, enabling researchers to look in greater detail at the physical processes connecting different parts of the climate system. To date, the U.S. National Climate Assessment as well as the Intergovernmental Panel on Climate Change (IPCC) have considered only a limited number of processes in their attempts to understand observed climate trends and to make projections about possible future climate scenarios. One of the potentially important issues that Pielke (2002) raises is the impact of anthropogenic land cover change on climate. Pielke et al. (1998) discuss the many short- and long-term processes that connect the terrestrial ecosystem and overlying atmosphere; they assert that, "In studies of past and possible future climate change, terrestrial ecosystem dynamics are as important as changes in atmospheric dynamics and composition, ocean circulation, ice sheet extent, and orbital perturbations" (460–4611). We use the Geophysical Fluid Dynamics Laboratory (GFDL) climate model to test the hypothesis that alterations to the vegetation cover of the earth's surface due to human activities have altered regional

Corresponding author address: Kirsten L. Findell, NOAA/Geophysical Fluid Dynamics Laboratory, 201 Forrestal Rd., Princeton, NJ 08540.
E-mail: kirsten.findell@noaa.gov

DOI: 10.1175/JCLI4185.1

and global climates through biophysical influences. This study does not consider the impact of ecosystem dynamics and biogeochemical feedbacks on the climate system.

Recent studies have analyzed the influences of observed land cover changes on climate using atmosphere-only general circulation models (Bonan 1999), coupled atmosphere–slab ocean general circulation models (Bounoua et al. 2002; Govindasamy et al. 2001; Zhao and Pitman 2002), and earth system models of intermediate complexity (EMICs; Claussen et al. 2003; Matthews et al. 2003; Brovkin et al. 2004). Feddema et al. (2005) stress the importance of including projections of land cover change in simulations of future climates, as well. Land cover feedbacks are typically separated into biogeochemical and biophysical processes. Biogeochemical influences are associated with changes in the net carbon uptake by plants and soils and tend to have positive feedbacks on climate (Friedlingstein et al. 2003). As noted above, these influences are not considered in this study. Biophysical influences are typically caused by changes in the radiative properties of the land surface (e.g., albedo) and the properties directly affecting the surface water budget and turbulent exchanges (e.g., root and stomatal properties, roughness length). Govindasamy et al. (2001) and Matthews et al. (2003) reported local and regional cooling resulting from albedo increases associated with anthropogenic conversion of midlatitude forests to agriculture, particularly in winter. Bonan (1997, 1999) and Oleson et al. (2004) reported summer cooling caused by midlatitude deforestation and attributed the cooling to changes in stomatal conductance. Zhao et al. (2001) and Zhao and Pitman (2002) report cooling in some midlatitude regions and warming in other regions in response to conversion from natural to present-day land cover; they suggested that a suite of parameter changes associated with the land cover change was responsible for the surface temperature changes. In general, the magnitude, location, and direction of the changes in turbulent fluxes vary among the studies, particularly in summer months, and appear to be dependent on the specifics of the land model parameterizations.

A brief description of our model and experiments is provided in the next section of this work. A discussion of the physical processes influenced by vegetation parameters is given in section 3. In section 4 we describe the results from a global perspective, and in section 5 we focus on regions where the vegetation types changed between the experiments. Discussion of the results and comparisons with surface temperature observations are provided in section 6, and the conclusions are presented in section 7.

2. Model description and experimental design

The equilibrium climate model used for the experiments described below comprises an atmospheric general circulation model coupled to a 50-m-deep slab or "mixed layer" model of the ocean. The model grid cells are 2.5° longitude by 2° latitude in all model components with 24 vertical levels in the atmosphere. The model has a seasonal and a diurnal cycle of insolation. The model's treatment of the atmosphere, land, and sea ice is the same as that in the Climate Model version 2.0 (CM2.0) model presented by Delworth et al. (2006). The details of the atmospheric component and the fidelity of its performance are contained in a paper from the GFDL Global Atmospheric Model Development Team (2004, hereafter GAMDT04). GAMDT04 and Milly and Shmakin (2002a) describe the land component in detail; in section 3 we discuss the land model parameters that are altered with land cover change. The slab ocean component is coupled to a dynamic/thermodynamic sea ice subcomponent (Winton 2000; additional model documentation is available from the GFDL Web site at http://nomads.gfdl.noaa.gov.)

The pair of experiments presented here consisted of a 100-yr integration with land cover set to 1990 conditions (referred to as the All1990 run) and a 60-yr integration in which the land cover was changed to reflect the potential natural vegetated state (described below; NatVeg run). Both simulations had time-invariant concentrations of atmospheric greenhouse gases and other radiative forcing constituents fixed at 1990 levels [see Knutson et al. (2006) for details on the various forcings used in these model integrations]. The only difference between the simulations is the imposed land cover distribution. Analyses were conducted on the last 50 years of the two integrations.

The potential natural land cover distribution (Fig. 1a) approximates the land cover conditions that would exist in the absence of human disturbance. It is based on the Milly and Shmakin (2002a) classification that was part of the Land Dynamics model (LaD). LaD has 10 vegetation types that are groupings of the 32 Matthews vegetation types (Matthews 1983). The LaD vegetation types include broadleaf evergreen, broadleaf deciduous, mixed forest, needle-leaf deciduous, needleleaf evergreen, grassland, desert, tundra, and ice. Parameter values for each of these cover types are listed in Table 1. Milly and Shmakin (2002a) include an agriculture type in the LaD code, but parameter values for this type are highly uncertain and have not been tested. In this work, we use the grassland type to represent crops and/or pastures. Other studies (e.g., Hansen et al. 1998; Matthews et al. 2003) have used this same ap-

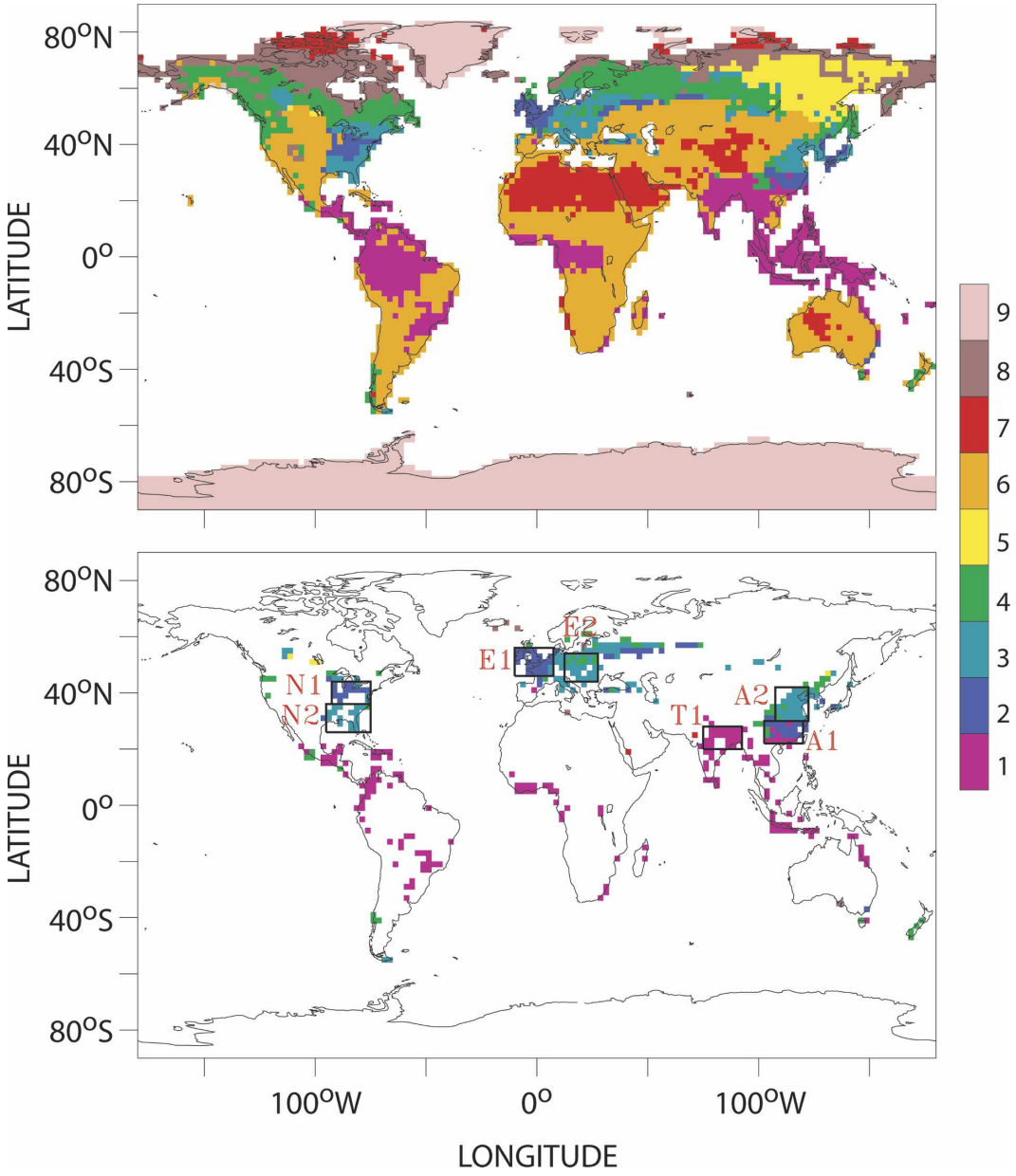

FIG. 1. (top) Cover types for the NatVeg simulation, 1: broadleaf evergreen, 2: broadleaf deciduous, 3: broadleaf/needleleaf, 4: needleleaf evergreen, 5: needleleaf deciduous, 6: grassland/crops/pasture, 7: desert, 8: tundra, and 9: glacier. (bottom) All1990 − NatVeg differences in cover type; 11.6% of the land surface is converted to grasslands. Colors in (bottom) are representative of the original cover type shown in (top). Boxes in (bottom) are used to indicate regions used in analyses and discussion later in the paper, North American boxes: N1 and N2; European boxes: E1 and E2; Asian boxes: A1 and A2; and tropical box: T1.

proximation. Some observational studies also provide support for this assumption. Mahmood and Hubbard (2002), for example, show that nonirrigated crops and natural grasslands in Nebraska (central United States) produce similar fluxes of heat and moisture. LaD prescribes a single dominant vegetation type for each grid cell and, therefore, does not represent subgrid-scale heterogeneity.

The 1990 land cover type distribution was derived by combining the potential vegetation distribution described above with the reconstruction of global land use history detailed by Hurtt et al. (2006). Figure 1b shows the differences between the natural and 1990 cover-type maps; 11.6% of the earth's land surface differs (was converted from native forests to grassland) between the two cover type distributions. Additionally,

TABLE 1. Minimum bulk NWS stomatal resistance (s m^{-1}), effective rooting depth (m), snow-free albedo (-), roughness length (m), and the critical snowmass (kg m^{-3}; the snow amount that covers half of the surface) used in momentum and surface flux calculations for land cover types used in the GFDL land surface model.

	NWS stomatal resistance (s m^{-1})	Effective rooting depth (m)	Snow-free albedo	Roughness length (m)	Critical snowmass (kg m^{-3})
1 (BE) broadleaf evergreen trees	43.6	1.30	0.149	2.65	60
2 (BD) broadleaf deciduous trees	131.0	1.38	0.130	0.90	10
3 (BN) broadleaf/needleleaf trees	87.1	1.61	0.132	1.20	25
4 (NE) needleleaf evergreen trees	69.7	0.84	0.126	0.90	40
5 (ND) needleleaf deciduous trees	218.0	0.84	0.143	0.80	40
6 (G) grassland	56.6	0.98	0.182	0.07	5
7 (D) desert	0.0	1.00	0.333	0.01	5
8 (T) tundra	170.0	0.49	0.139	0.07	5

according to the Hurtt et al. (2006) database, transitions from natural grasslands to crops or pastures occurred on about 15% of the land, but these transitions do not show up in Fig. 1 due to our treatment of grassland, crops, and pastures as one cover type. This estimate of land area converted from a potential, undisturbed state to crops or pastures is within the range of similar estimates provided by other studies (Vitousek et al. 1997; Ramankutty and Foley 1999; Chase et al. 2000; Pitman and Zhao 2000; Klein Goldewijk 2001).

3. A conceptual framework

To facilitate the discussion of the physical processes modeled in studies of land cover change, a general schematic is provided in Fig. 2 for the example of conversion from forest to grassland. As discussed in detail below, changes in land cover lead to changes in parameters controlling the use of available water and energy at the surface. In the LaD scheme, altered surface parameters include the rooting depth, non-water-stressed (NWS) bulk stomatal resistance, surface roughness length, snow-free surface albedo, and snow-masking depth. These model-prescribed parameters are shown in bold in Fig. 2, with increases and decreases associated with the parameterization implemented in the GFDL model. Values of each of these parameters are listed in Table 1 for each of the cover types (see Milly and Shmakin 2002a for more details). Figure 3 maps differences resulting from parameter changes between the All1990 and the NatVeg simulations. The rooting depth is directly related to the water-holding capacity of the root zone shown in Fig. 3, and the snow-masking depth is directly related to the critical snowmass (the snow amount that hides half the surface) listed in Table 1.

Three model-prescribed parameters directly influence the hydrologic cycle through their influence on evapotranspiration (E): the rooting depth, the roughness length, and the non-water-stressed bulk stomatal resistance (top-left side of Fig. 2). Decreases in the rooting depth effectively reduce the maximum water-holding capacity (the soil moisture reservoir size) of the grid cell. For a given rainfall event, a small soil moisture reservoir is more likely to saturate than a large reservoir, so precipitation is more likely to be removed by surface runoff, leaving less moisture available for evapotranspiration. Decreases in the roughness length (grasslands typically are shorter than forests) lead to decreases in turbulent mixing in the boundary layer and decreased evapotranspiration, although the effect is small in the model. Changes in the non-water-stressed bulk stomatal resistance (effectively including changes in leaf-scale stomatal resistance and leaf area) influence the ease with which water can pass from the plant to the atmosphere: increased resistance results in less evapotranspiration in the model.

For the LaD parameter settings used in the GFDL model, changes of any one of these three parameters lead to decreased evapotranspiration in the Tropics when forests are converted to grasslands. Where midlatitude forests are replaced with grasslands, decreased stomatal resistance increases evapotranspiration, while the roughness length and rooting depth changes reduce evapotranspiration through similar processes as those operating in the Tropics. As will be discussed in the next two sections, the net effect of these changes is decreased evapotranspiration in most regions in the GFDL model.

Other parameters altered in most studies of land cover change impact the surface albedo. In the GFDL model, the relevant parameters are snow-free albedo and snow-masking depth (top right of Fig. 2). When forests are converted to grasslands, the snow-free albedo increases and the snow-masking depth decreases. The effect of the former parameter change is to increase the surface albedo year-round in tropical regions and during periods with no snow cover in middle and high latitudes. The effect of the latter parameter change

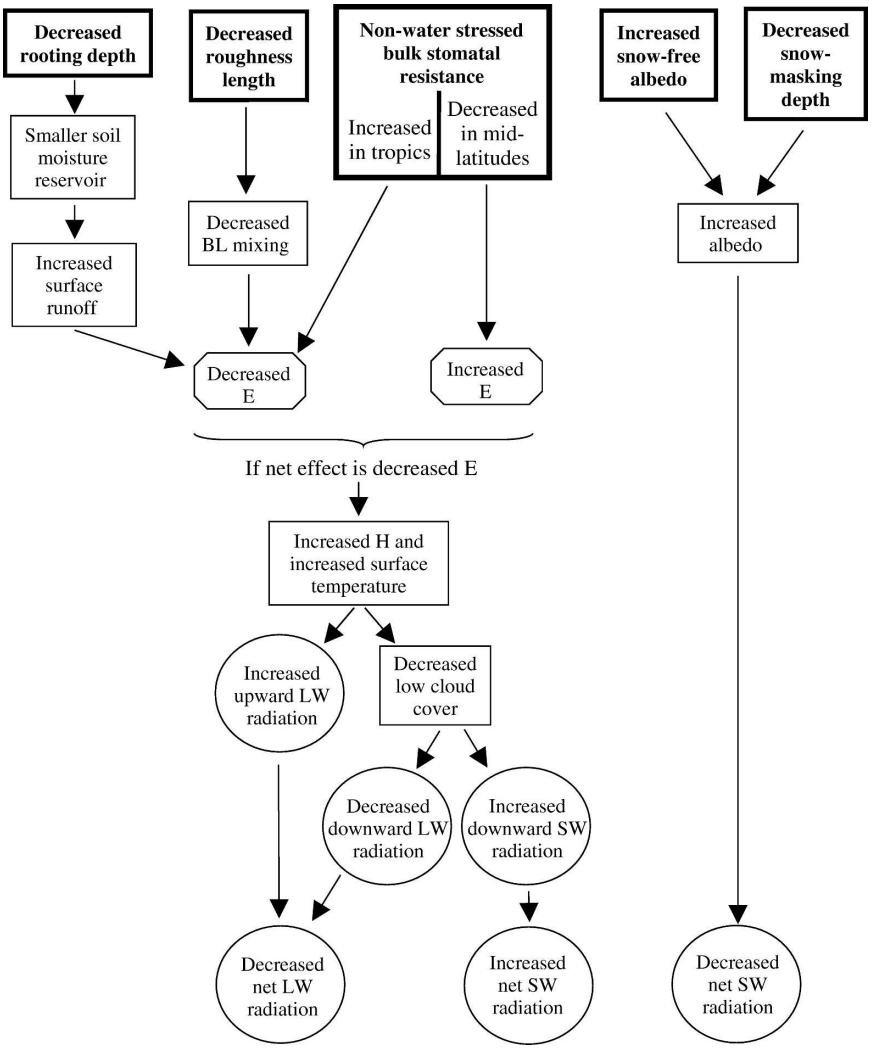

FIG. 2. Idealized schematic of physical processes influenced by the conversion of forests to grasslands. Model-prescribed physical parameters are in bold; BL: boundary layer, *E:* evapotranspiration, *H*: sensible heat flux, LW: longwave, and SW: shortwave. All radiative fluxes (in circles) are surface fluxes (positive toward the surface).

is to increase the surface albedo when snow is present. Thus, both parameter changes lead to increases in surface albedo, particularly in snowy regions. The more reflective surface means that less incoming shortwave radiation is absorbed by the surface, making less energy available for sensible and latent heating. Surface albedo is not directly impacted by soil moisture in the model.

Figure 2 also shows, however, that the surface radiation balance is complicated by feedbacks resulting from changes in the partitioning of available energy into latent and sensible heating (λE and H, respectively, where λ is the latent heat of vaporization). If the direct hydrological effects in the top-left corner of Fig. 2 (discussed above) lead to a net decrease in evapotranspiration, as is the case in these experiments, then more energy is available for sensible heat flux and the surface temperature (T_{surf}) increases. The decrease in latent heat flux and increases in sensible heat flux and surface temperature are accompanied by a decrease in low cloud cover resulting from the increased buoyancy and decreased moisture content of the near-surface atmosphere. The increased surface temperature is accompanied by an increase in the amount of longwave (LW) radiation leaving the earth's surface and, because of the reduced low cloud cover, less of this radiation is returned to the surface. These two effects yield a decrease in net longwave radiation at the surface. However, the decreased low cloud cover also allows more incoming shortwave radiation to reach the surface. The increase in downward shortwave radiation at the surface, how-

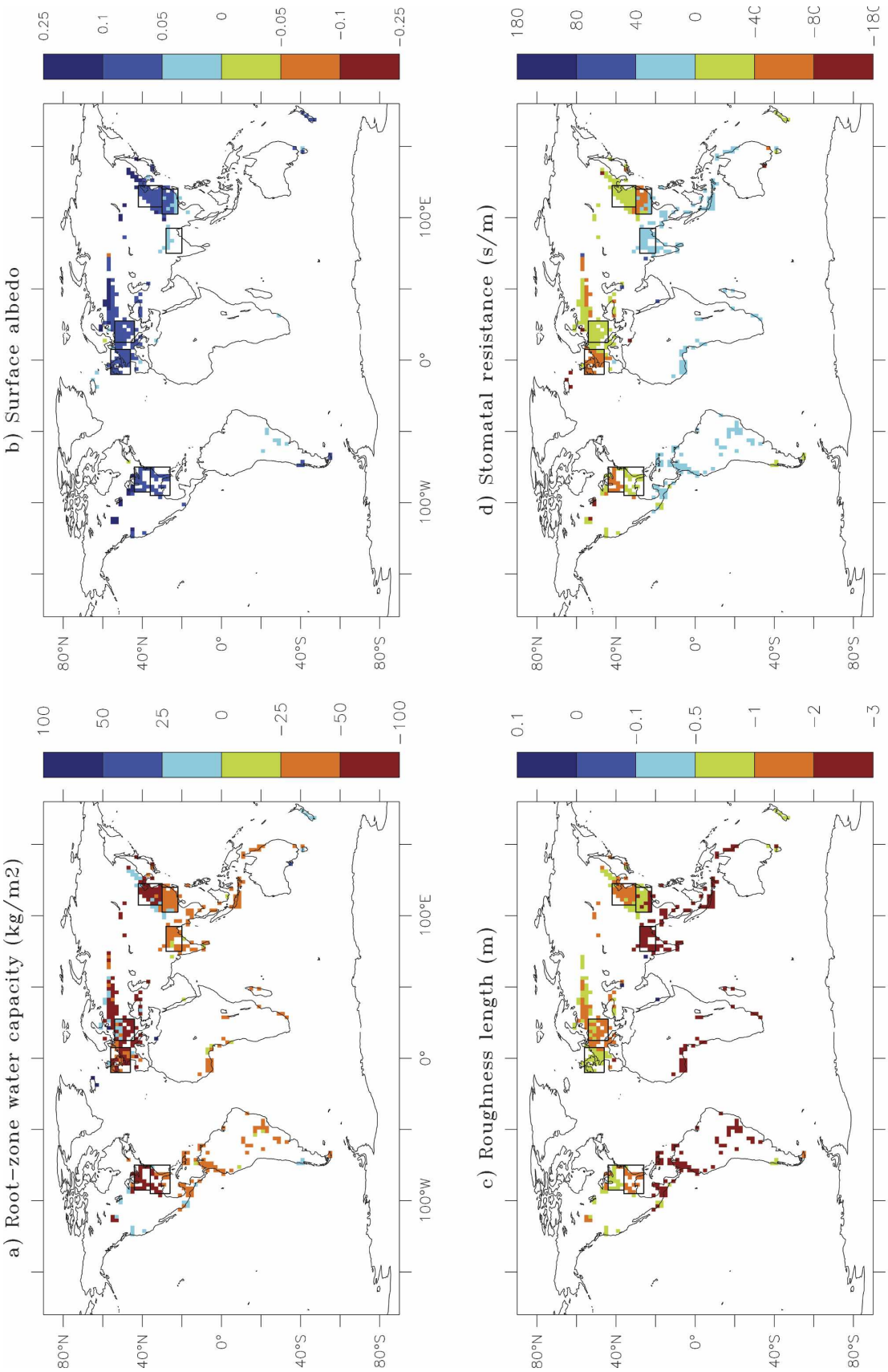

FIG. 3. Surface changes in (a) root-zone water holding capacity (kg m^{-2}), (b) surface albedo, (c) roughness length (m), and (d) stomatal resistance (s m^{-1}) resulting from the prescribed land cover conversion. Differences are All1990 − NatVeg. Note that albedo changes reflect differences in snow-free albedo, snow-masking depth, and snow cover between the two runs; albedo changes are only shown in the regions with land cover conversion. Boxes are the same as in Fig. 1b.

ever, is opposed by a decrease in absorbed shortwave radiation resulting from the changes to surface albedo discussed above and shown on the far right of Fig. 2. If the net surface radiative balance (bottom line of Fig. 2) is negative, then both latent and sensible heat fluxes may decrease, and surface temperatures may also decrease.

Precipitation responses to parameter changes are not included in Fig. 2 because of the variety and complexity of relevant feedbacks between atmospheric and surface processes and the small precipitation response found in our experiments. For convective rainfall to occur, a lifting mechanism and atmospheric moisture must both be available. Sensible heat flux can contribute to the former requirement and latent heat flux can contribute to the latter requirement. Thus, one cannot always easily deduce how changes in the partitioning of these surface fluxes and changes in the availability of surface radiation will influence precipitation. Findell and Eltahir (2003a,b) show that the precipitation response to changed surface fluxes is dependent on local atmospheric conditions and that some regions are more likely to see increased convection when latent heat flux increases and other regions are more likely to see increased convection when sensible heat flux increases.

Given the processes and interactions sketched out above, model results are highly sensitive to the parameter settings and to the relative strengths of various processes within a given land surface model. For example, the GFDL model shows modest summertime warming in midlatitude regions converted from forests to agriculture (discussed below), although Bonan (1997, 1999) simulated summer cooling of 1°C in the central United States using a version of the National Center for Atmospheric Research (NCAR) Community Climate Model version 2 (CCM2) with the Land Surface Model version 1 (LSM1). Oleson et al. (2004) found similar summer cooling with LSM1, but they found that simulations with a warmer and drier land surface model (CLM2) had smaller summer cooling. In contrast, the results of Xue et al. (1996) showed a warmer summertime climate when crops occupied the central United States than when these crops were replaced with trees. Zhao et al. (2001) found little change in North American response to similar land cover change using NCAR's CCM3 coupled to the Biosphere–Atmosphere Transfer Scheme (BATS), but they found cooling in Europe, India, and northern China and warming in southern China in this study and the follow-up study by Zhao and Pitman (2002).

In view of the foregoing discussion, it is clear how experimental results depend critically on the fidelity of a model's representations of the relative strengths of interacting processes like those included in Fig. 2. However, this fidelity is difficult to assess. The dearth of reliable datasets for land-model parameters, fluxes, and states greatly impedes the assessment of the realism of any model's sensitivity to land cover. A small measure of confidence in the vegetation dependence of parameters used in this study is gained from the work of Milly and Shmakin (2002b). Milly and Shmakin sought to determine if specification of parameters on the basis of global soil and vegetation distributions improved model performance over that with globally constant parameters. Their results showed that model performance—as measured by the prediction of annual runoff ratios of large river basins—did indeed improve when parameters were tied to soil and vegetation characteristics in the LaD model. Additional motivation for performing this study with the GFDL model is provided by the results of the Global Land–Atmosphere Coupling Experiment (GLACE; Koster et al. 2006; Guo et al. 2006); this model intercomparison project quantified the land–atmosphere coupling strength of 12 atmospheric general circulation models. Coupling strength is defined in GLACE as "the degree to which anomalies in land surface state (e.g., soil moisture) can affect rainfall generation and other atmospheric processes" (Koster et al. 2006, p. 590). Koster et al. show that the GFDL model is among the models with the strongest land–atmosphere coupling strength.

4. Global sensitivity

Difference fields (All1990 − NatVeg) for a few variables are shown in Figs. 4–6, and Table 2 lists annual average global differences for these and other variables. These differences are small in magnitude; although some are statistically significant [column (a)], they tend to be within one standard deviation of the mean values observed in the NatVeg experiment [column (b)] and would be hard to distinguish from normal climate variability on short time scales. This result is consistent with other studies that have shown a lack of sensitivity in global averages in response to similar land surface perturbations (Chase et al. 2000; Zhao et al. 2001; Bounoua et al. 2002).

Additionally, all fields listed in Table 2 show only 3%–7% of the earth's surface passing a modified Student's t test at the 95% significance level. The modified test accounts for autocorrelation of the time series (Zwiers and von Storch 1995; von Storch and Zwiers 1999). The t test does not address field significance. Field significance tests require estimates of the numbers of spatial degrees of freedom (DOF) for each vari-

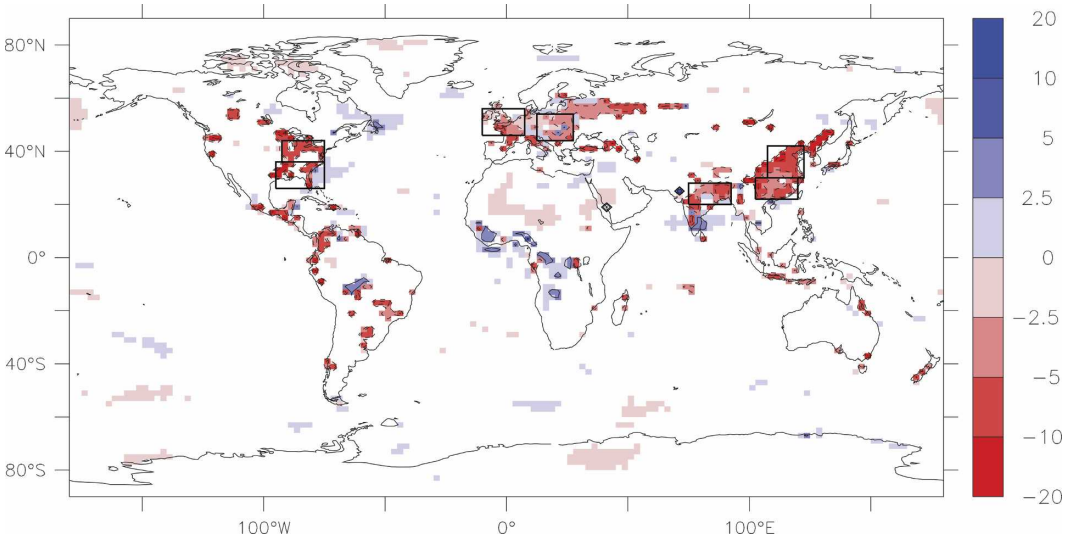

FIG. 4. Annual difference in net radiation at the surface (All1990 − NatVeg). Differences are shaded only where statistically significant at the 95% significance level according to the modified *t* test, but they are contoured everywhere (0.0 contour line not included). 6.5% of global area passes this test. Boxes are the same as in Fig. 1b.

able (see, e.g., Livezey and Chen 1983) tested. Variables with large correlation lengths (e.g., temperature) have fewer DOF than variables with short correlation lengths (e.g., precipitation) and therefore require much more than 5% of the area to pass the 95% significance level test for the whole field to be deemed statistically significant. Livezey and Chen (1983) show that fields with only 7% of area passing a 95% significance test (the maximum listed in Table 2) require more than 400 DOF to achieve field significance at the 95% significance level. DOF estimates depend on the variable and the time scale of interest (daily, seasonal, annual), but DOF estimates for global scale, annually averaged fields like those listed in Table 2 tend to be smaller than 100 (see, e.g., Van den Dool and Chervin 1986). Fields with 100 DOF require more than 9% of the area to pass a 95% significance test for the field as a whole to be significant at the 95% level (Livezey and Chen 1983). Given that none of the global fields analyzed here exceeded about 7% passing the modified 95% level *t* test,

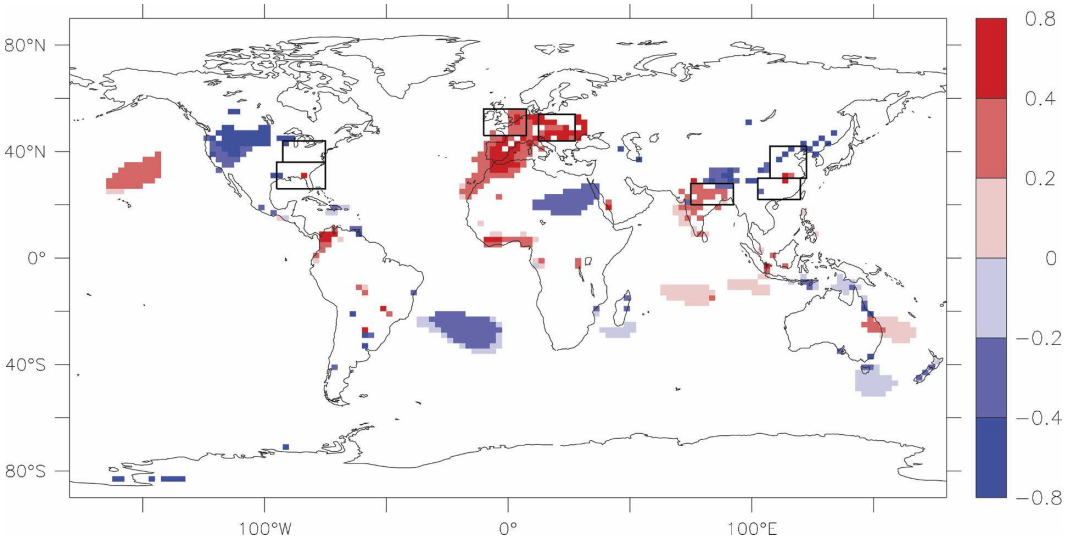

FIG. 5. As in Fig. 4 but for 2-m air temperature differences (1990 − NatVeg); 6.0% passes at the 95% significance level.

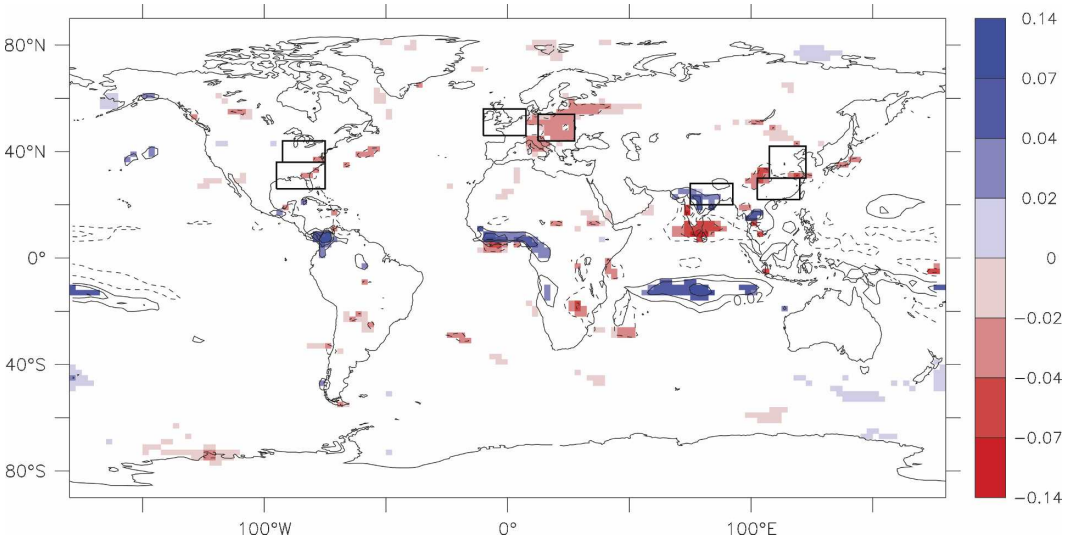

FIG. 6. As in Fig. 4 but for precipitation differences (1990 − NatVeg). 3.9% passes at the 95% significance level.

a more rigorous assessment of field significance was not performed.

5. Regional sensitivity

Although we do not see large changes from a global perspective, the prescribed alterations to surface vegetation cover lead to some substantial changes in many of the regions where land cover change occurs. Figure 7 summarizes some annual average differences for a subset of regions that have undergone extensive land cover change (Fig. 1b), and Figs. 8 and 9 show the seasonal cycles of many variables for the regions of eastern Europe (E2) and northern India (T1), respectively.

In all of the regions shown in Fig. 7a, annual average evapotranspiration is significantly reduced. This is even true in each of the midlatitude regions where there are competing impacts of the prescribed land cover change on the calculated evapotranspiration (Fig. 2). All regions also show an increase in surface runoff (R) associated with the decreased rooting depth and accompanying the decreased evapotranspiration, with the exception of eastern Europe (E2) where runoff is unchanged. Figure 7a also shows small decreases in annual precipitation in all of the temperate regions and a small increase in the tropical region of northern India (T1). Regions E2 and T1 showed the largest annual mean changes; Figs. 8b and 9b show the seasonal cycles

TABLE 2. (a) Global mean differences (All1990 − NatVeg) of annual average values; (b) standard deviation of annual global mean values within the NatVeg run; and (c) passing percentages for many variables. Bold type in column (a) indicates statistically significant differences.

Variable	(a) Global mean difference (All1990 − NatVeg)	(b) Std dev of annual global mean value in NatVeg run	(c) Percent of globe* passing modified 95% Student's t test
Precipitation (P: cm day^{-1})	**−0.0008**	0.0009	3.9%
Evaporation (E: cm day^{-1})	**−0.0008**	0.0009	6.5%
Surface runoff (only defined on land: cm day^{-1})	**0.0015**	0.0016	7.3%*
Sensible heat flux (H: W m^{-2})	**0.0967**	0.1537	5.5%
2-m air temperature (°C)	0.0080	0.0626	6.0%
Low cloud amount (%)	**−0.2499**	0.1889	5.2%
Net surface shortwave radiation (W m^{-2})	0.1198	0.2976	5.3%
Net surface longwave radiation (W m^{-2})	**−0.2639**	0.2267	5.1%
Net surface radiation (W m^{-2})	**−0.1441**	0.2036	6.5%
Net radiation at the top of the atmosphere (W m^{-2})	−0.0121	0.2620	6.7%

* Surface runoff is calculated only on land: for this variable, the percentage passing in column (c) is the percent of land area passing.

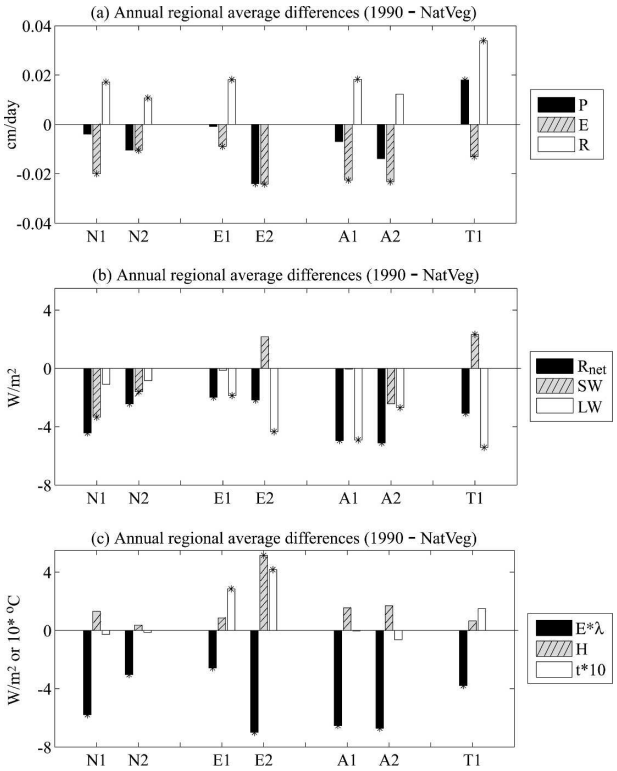

FIG. 7. Annual regional average differences (All1990 − NatVeg) for (a) variables involved in the water balance (precipitation, evaporation, and surface runoff), (b) variables involved in the surface radiation balance (net, shortwave, and longwave radiation), and (c) surface fluxes and temperature (E*: latent heat flux, H: sensible heat flux, and t*10: 2-m air temperature scaled by a factor of 10). The asterisks at the end of some bars indicate differences that are significant within the indicated region at the 95% level according to the modified *t* test of von Storch and Zwiers (1999). Region labels correspond to boxes indicated oi Fig. 1b.

of precipitation for these regions in both the NatVeg and the All1990 integrations.

The impacts of deforestation on the surface radiation balance include direct effects resulting from changes to the surface albedo and indirect effects following atmospheric feedbacks (Fig. 2). Consistent with the schematic in Fig. 2, the net longwave (LW) response is negative in all the regions highlighted in Fig. 7b, though the change is not statistically significant in the two North American regions (N1 and N2). The combination of decreased net shortwave (SW) radiation resulting from albedo changes and increased net shortwave radiation resulting from the decrease in low cloud cover following the decrease in evapotranspiration yields decreases in net shortwave radiation in three of the seven regions shown in Fig. 7b, increases in two regions, and essentially no change in the other two regions. In all regions the total available radiation at the surface, R_{net}, is lower in the All1990 run than in the NatVeg run.

Decreases in latent heat flux are generally accompanied by increases in sensible heat flux (Fig. 7c), though due to the competing influence of decreased net radiation at the surface, the increased sensible heat flux is only significant in eastern Europe (E2). Given that many of the changes shown in Figs. 4–7 are significant in region E2, Fig. 8 is included to highlight the seasonal cycles of many variables in this region and to better illustrate the physical processes at work.

Evidence of many of the physical processes and interactions among those processes discussed in section 3 are seen in seasonal cycles for the E2 region where the land cover was changed from the mixed broadleaf/needleleaf forests in the NatVeg simulation to grasslands in the All1990 simulation (Fig. 8). The reduction of root zone soil moisture is relatively stable throughout the year and averages about 40 kg m^{-2}. Evaporation (E) and precipitation (P) are also decreased throughout the year (Fig. 8b). As a result of the near balance between reduced evapotranspiration and precipitation, runoff does not change appreciably.

Changes to the surface radiation balance (Fig. 8c) are also consistent with the schematic in Fig. 2: a change from native forests in the NatVeg simulation to grassland in the All1990 simulation leads to decreased net longwave radiation throughout the year, increased shortwave radiation during the summer months, and decreased shortwave radiation during the winter months. The shortwave radiation changes suggest that the cloud effects dominate the shortwave radiation balance in the summer, but the surface albedo effects dominate in winter. The shortwave and longwave effects nearly cancel in the summer months, but the annual effect on net radiation at the surface, R_{net}, is a significant reduction (Fig. 7b) due to the wintertime increase in surface albedo. The evapotranspiration reduction discussed above is seen again in Fig. 8d in the form of reduced latent heat flux (λE). This is accompanied by increased sensible heat flux (H), with maximum differences in August. Surface temperature differences tend to be largest in the summer months (Fig. 8a).

The region of northern India (T1) is included in Fig. 7 and highlighted in Fig. 9 as an example of a region where tropical forests were converted to grasslands. The other areas with such a land cover conversion (Fig. 1b) tend to be smaller or have fewer adjacent altered grid cells. Northern India and many of the other tropical areas differ from extratropical regions in that the soils in northern India almost completely dry out for at least a few months of the year (Fig. 9a), yielding energy

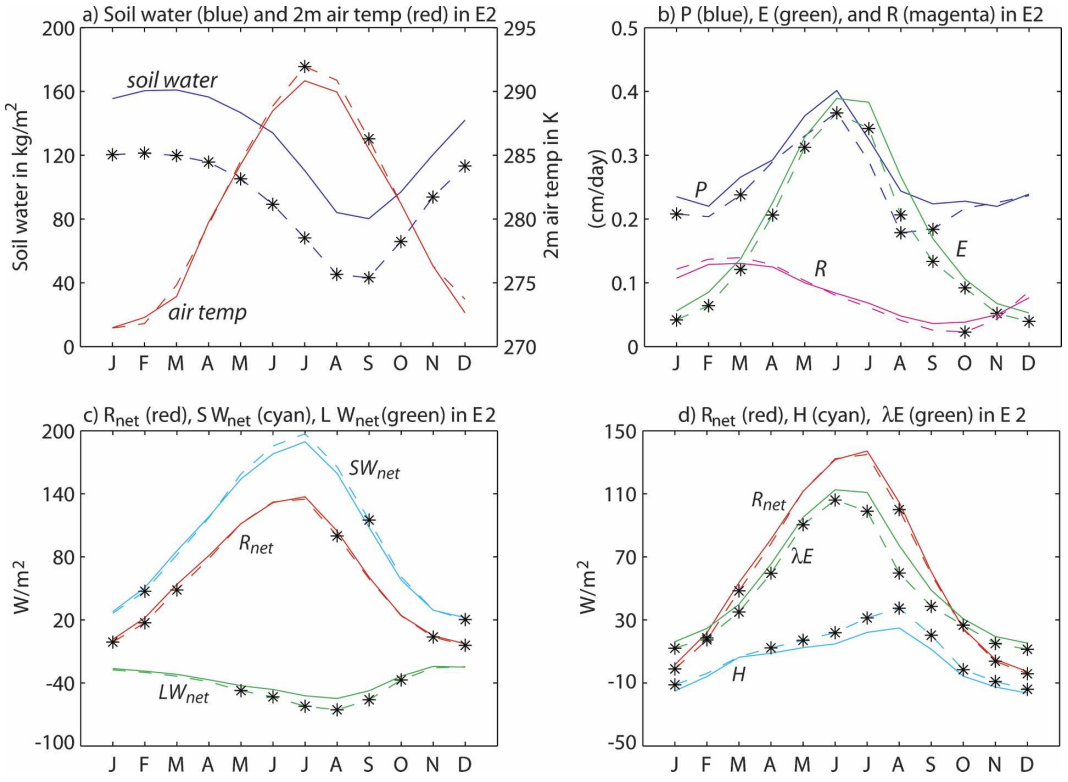

FIG. 8. Seasonal cycles averaged over eastern Europe (Region E2; 44°–54°N, 12.5°–27.5°E) for the NatVeg run (solid lines) and the All1990 run (dashed lines) of (a) root-zone soil moisture and 2-m air temperature; (b) precipitation (P), evaporation (E) and runoff (R); (c) net, shortwave, and longwave radiation at the surface (R_{net}, SW_{net}, and LW_{net}, respectively); and (d) R_{net} with sensible (H) and latent (λE) heat fluxes from the surface. Asterisks indicate monthly differences that are statistically significant at the 95% level according to the modified t test.

and water cycles that are very different during wet and dry seasons. During the dry season, the decreased water-holding capacity associated with removal of native forests does not influence the water and energy budgets because the soils are already so dry and evapotranspiration is already close to zero (Fig. 9b). The increased surface albedo, however, does yield significant changes: shortwave and net radiation go down during the dry season (Fig. 9c). Because there is already almost no evaporation, this reduction in available energy translates into reductions in sensible heat flux, surface temperatures, and net longwave radiation at the surface (Fig. 9).

During the wet season, on the other hand, both the hydrologic and the radiative processes sketched in Fig. 2 are relevant. The prescribed change from tropical forests to grassland in northern India leads to less evaporation, more runoff, more sensible heat flux, higher surface temperatures, fewer clouds, more shortwave radiation, and less net longwave radiation (Fig. 9). These radiation changes typically result in no change in net radiation at the surface during these wet season months. In the model, the annual effects in the T1 region are dominated by the wet season behavior (Fig. 7).

Sensitivities of surface fluxes and related variables to land cover change in regions like northern India may be substantially biased in our model. Milly and Shmakin (2002a) identified a bias in interseasonal water storage in the LaD model in regions where climatic aridity is strongly seasonal. The model does not account for upward diffusion of deep soil water during the long dry season or for evapotranspiration from areas of groundwater discharge. Such processes can contribute nonnegligibly to latent heat flux and limit sensible heat flux during the dry season.

6. Historical perspective

To put these changes into perspective, we compare the climatic changes observed over the past century or so with our experimental results. Such a comparison is useful because it helps quantify the contribution of anthropogenic land cover change to observed climate trends. However, the comparison must be interpreted

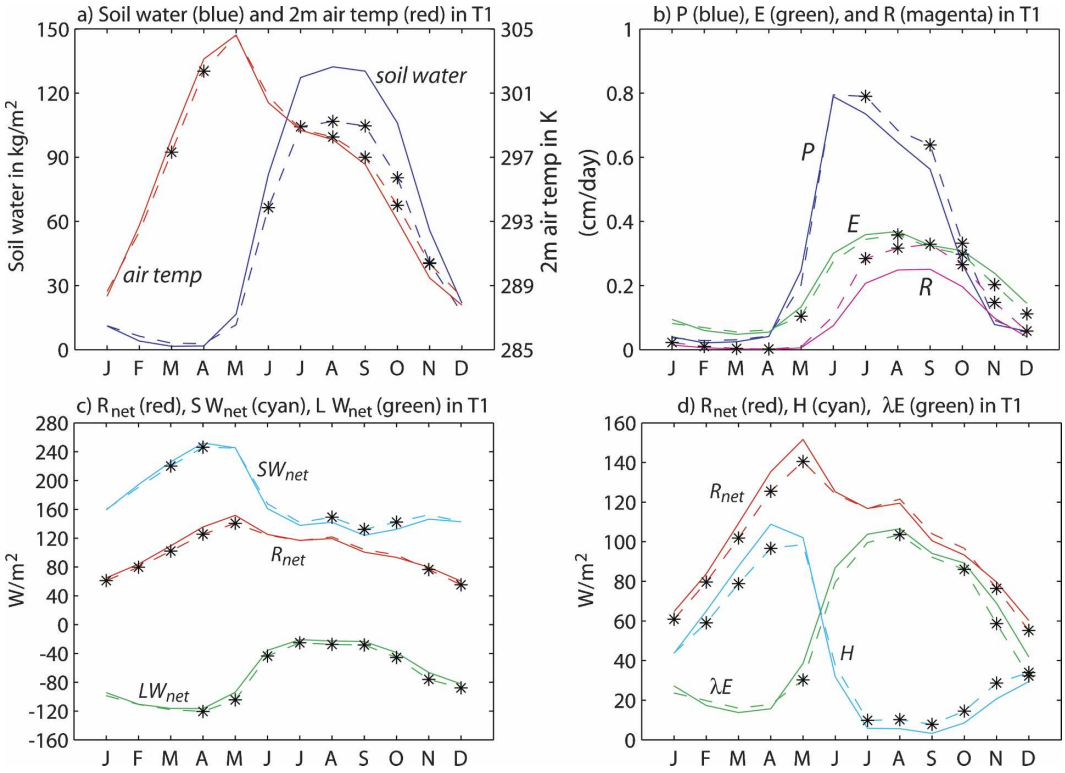

FIG. 9. As in Fig. 8 but for the region of northern India (Region T1: 20° to 28°N, 75° to 92.5°E).

with a number of caveats in mind. First, the model results are from an equilibrium calculation in which the climate system is given a sufficient amount of time to adjust fully to the prescribed changes. The observations are taken from time-dependent changes observed in the real world from the 1870s to the present (discussed below). An equilibrium experiment would be expected to show larger responses to perturbations than a transient experiment because the simulations, by definition, have equilibrated with the forcings while the real world is not in equilibrium (Hansen et al. 2005; Wetherald et al. 2001). Additionally, our equilibrium experiments account for changes to land surface cover that have accumulated since humans first began to modify the face of the land through agriculture and other activities; we are comparing a potential vegetation state (no human disturbance) to the present-day condition. Not all impacts resulting from these changes would be captured by a time series of the most recent 130 years. These two factors suggest that our experiments place an upper bound on the potential impact of the biophysical effects of anthropogenic land cover change. Thus, if land cover change was the major cause of observed climate changes, we would expect to see a larger signal in the model differences than in the observed differences. In reality, many additional forcing factors have changed in the real world since 1870 (and before) such as greenhouse gas and aerosol concentrations, solar insolation, and other factors (Hansen et al. 1998). We make the following comparison simply to give some perspective on the magnitude of the temperature changes simulated by our model.

We use observations from the Hadley Centre Climatic Research Unit Temperature version 2 (HadCRUT2v) surface temperature dataset [see Jones and Moberg (2003) for treatment of land-based data; Rayner et al. (2003) for treatment of ocean-based data; and Jones et al. (2001) for details on the variance adjustment method for dealing with differing spatial and temporal data density] to estimate surface temperature changes since the 1870s in each of the labeled regions in Fig. 1b. The black bars in Fig. 10 represent the regional differences between the observed surface temperature in the last 20 years and the first 20 years of the observational record (1985–2004 versus 1871–90). The white bars in Fig. 10 represent the differences between the 50-yr climatologies of the All1990 run and the NatVeg run of our equilibrium climate model for the regions indicated in Fig. 1b. These regions are the areas where the land cover was changed in the model integrations and where the resulting climate response is the largest. If different regions were considered, the model signal (i.e., the

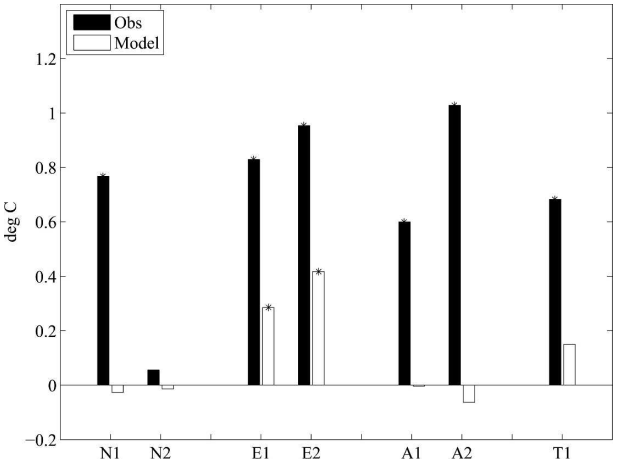

FIG. 10. Black bars: for each region, observed temperature differences from the HadCRUT2v dataset, average of 1985–2004 minus average of 1870–89. Asterisks on black bars indicate that the temperature trends from 1870 to 2004 are significantly different from 0 at the 99.9% significance level in every region except N2. White bars: for each region, modeled temperature differences between the 50-yr averages of the All1990 run and the NatVeg run. Asterisks on white bars indicate regions where the modeled differences between the All1990 and the NatVeg runs are significant at the 95% significance level (modified *t* test).

white bars in Fig. 10) would be smaller. Even in these regions, where the land cover change effect is largest, the model difference between the All1990 run and the NatVeg run is much smaller than the observed warming over the last 130 years in the North American, Asian, and tropical regions. In the European regions the simulated surface temperature differences are a sizable fraction of the observed trends. However, they still are less than about 40% of the observed signal. This leads us to conclude that, though land cover changes can have significant impacts on regional water and energy balances, the observed surface warming in the real world cannot be explained by land cover change alone and that other changes in radiative forcing are collectively playing a much more dominant role.

7. Conclusions

According to the GFDL equilibrium climate model, climatic impacts of anthropogenic land cover change have a small impact at the global scale but are climatically significant in a few regions, specifically eastern Europe, northern India, and eastern China. Regional impacts of land cover change are small in North America. Contrary to some previous studies on this topic (Zhao and Pitman 2002; Bonan 1999; Hansen et al. 1998), model-simulated annual surface temperature fields indicate that where differences exist between the present-day simulation and the simulation with potential natural vegetation cover, conditions are predominantly warmer as a result of anthropogenic land cover change. The surface warming is largest in Europe.

Observations of surface air temperature show warming across much of the globe over the past century (Houghton et al. 2001; Knutson et al. 2006). Comparisons of the results of the model integrations documented here with those observed temperature records indicate that anthropogenic land cover change is unlikely to be responsible for the observed global-scale warming. This conclusion is substantiated by the fact that, even in the regions where the effects of cumulative land cover change from a potential natural state to present-day conditions are large, the impact on surface temperatures is small relative to observed changes in surface temperatures over the last 130 years. Thus, within the limitations of the model, and noting that changes in water management practices (e.g., irrigation and impoundment of surface waters) and biogeochemical feedbacks of land cover changes are not included in the model, we can conclude that the biophysical impacts of anthropogenic land cover change are unlikely to be important drivers of observed global-scale climate change.

Acknowledgments. The authors thank Krista Dunne, Anand Gnanadesikan, Tom Delworth, and three anonymous reviewers for their helpful reviews of the manuscript.

REFERENCES

Bonan, G. B., 1997: Effects of land use on the climate of the United States. *Climatic Change,* **37,** 449–486.

——, 1999: Frost followed the plow: Impacts of deforestation on the climate of the United States. *Ecol. Appl.,* **94,** 1305–1315.

Bounoua, L., R. Defries, G. J. Collatz, P. Sellers, and H. Khan, 2002: Effects of land cover conversion on surface climate. *Climatic Change,* **52,** 29–64.

Brovkin, V., S. Sitch, W. Von Bloh, M. Claussen, E. Bauer, and W. Cramer, 2004: Role of land cover changes for atmospheric CO_2 increase and climate change during the last 150 years. *Global Change Biol.,* **10,** 1253–1266.

Chase, T. N., R. A. Pielke Sr., T. G. F. Kittel, R. R. Nemani, and S. W. Running, 2000: Simulated impacts of historical land cover changes on global climate in northern winter. *Climate Dyn.,* **16,** 93–105.

Claussen, M., and Coauthors, 2003: Earth system models of intermediate complexity: Closing the gap in the spectrum of climate system models. *Climate Dyn.,* **18,** 579–586.

Delworth, T. L., and Coauthors, 2006: GFDL's CM2 global coupled climate models. Part I: Formulation and simulation characteristics. *J. Climate,* **19,** 643–674.

Feddema, J. J., K. W. Oleson, G. B. Bonan, L. O. Mearns, L. E. Buja, G. A. Meehl, and W. M. Washington, 2005: The impor-

tance of land-cover change in simulating future climates. *Science,* **310,** 1674–1678.

Findell, K. L., and E. A. B. Eltahir, 2003a: Atmospheric controls on soil moisture–boundary layer interactions. Part I: Framework development. *J. Hydrometeor.,* **4,** 552–569.

——, and ——, 2003b: Atmospheric controls on soil moisture–boundary layer interactions. Part II: Feedbacks within the continental United States. *J. Hydrometeor.,* **4,** 570–583.

Friedlingstein, P., J.-L. Dufresne, P. M. Cox, and P. Rayner, 2003: How positive is the feedback between climate change and the carbon cycle? *Tellus,* **55B,** 692–700.

GFDL Global Atmospheric Model Development Team, 2004: The new GFDL global atmosphere and land model AM2–LM2: Evaluation with prescribed SST simulations. *J. Climate,* **17,** 4641–4673.

Govindasamy, B., P. B. Duffy, and K. Caldeira, 2001: Land use changes and northern hemisphere cooling. *Geophys. Res. Lett.,* **28,** 291–294.

Guo, Z., and Coauthors, 2006: GLACE: The Global Land–Atmosphere Coupling Experiment. Part II: Analysis. *J. Hydrometeor.,* **7,** 611–625.

Hansen, J. E., M. Sato, A. Lacis, R. Ruedy, I. Tegen, and E. Matthews, 1998: Climate forcings in the Industrial era. *Proc. Natl. Acad. Sci. USA,* **95,** 12 753–12 758.

——, and Coauthors, 2005: Earth's energy imbalance: Confirmation and implications. *Science,* **308,** 1431–1435.

Houghton, J. T., Y. Ding, D. J. Griggs, M. Noguer, P. J. van der Linden, X. Dai, K. Maskell, and C. A. Johnson, Eds., 2001: *Climate Change 2001: The Scientific Basis*. Cambridge University Press, 881 pp.

Hurtt, G. C., S. Frolking, M. G. Fearon, B. Moore III, E. Shevliakova, S. Malyshev, S. W. Pacala, and R. A. Houghton, 2006: The underpinnings of land-use history: Three centuries of global gridded land-use transitions, wood harvest activity, and resulting secondary lands. *Global Change Biol.,* **12,** 1208–1229.

Jones, P. D., and A. Moberg, 2003: Hemispheric and large-scale surface air temperature variations: An extensive revision and an update to 2001. *J. Climate,* **16,** 206–223.

——, T. J. Osborn, K. R. Briffa, C. K. Folland, B. Horton, L. V. Alexander, D. E. Parker, and N. A. Rayner, 2001: Adjusting for sampling density in grid-box land and ocean surface temperature time series. *J. Geophys. Res.,* **106,** 3371–3380.

Klein Goldewijk, K., 2001: Estimating global land use change over the past 300 years: The HYDE Database. *Global Biogeochem. Cycles,* **15,** 417–433.

Knutson, T. R., and Coauthors, 2006: Assessment of twentieth-century regional surface temperature trends using the GFDL CM2 coupled models. *J. Climate,* **19,** 1624–1651.

Koster, R. D., and Coauthors, 2006: GLACE: The Global Land–Atmosphere Coupling Experiment. Part I: Overview. *J. Hydrometeor.,* **7,** 590–610.

Livezey, R. E., and W. Y. Chen, 1983: Statistical field significance and its determination by Monte Carlo techniques. *Mon. Wea. Rev.,* **111,** 46–59.

Mahmood, R., and K. G. Hubbard, 2002: Anthropogenic land-use change in the North American tall grass–short grass transition and modification of near-surface hydrologic cycle. *Climate Res.,* **21,** 83–90.

Matthews, E., 1983: Global vegetation and land use data bases for climate studies. *Bull. Amer. Meteor. Soc.,* **64,** 793–794.

Matthews, H. D., A. J. Weaver, M. Eby, and K. J. Meissner, 2003: Radiative forcing of climate by historical land cover change. *Geophys. Res. Lett.,* **30,** 1055, doi:10.1029/2002GL016098.

Milly, P. C. D., and A. B. Shmakin, 2002a: Global modeling of land water and energy balances. Part I: The land dynamics (LaD) model. *J. Hydrometeor.,* **3,** 283–299.

——, and ——, 2002b: Global modeling of land water and energy balances. Part II: Land-characteristic contributions to spatial variability. *J. Hydrometeor.,* **3,** 301–310.

Oleson, K. W., G. B. Bonan, S. Levis, and M. Vertenstein, 2004: Effects of land use change on North American climate: Impact of surface datasets and model biogeophysics. *Climate Dyn.,* **23,** 117–132.

Pielke, R. A., Sr., 2002: Overlooked issues in the U.S. National Climate and IPCC assessments. *Climatic Change,* **52,** 1–11.

——, R. Avissar, M. Raupach, A. J. Dolman, X. Zeng, and A. S. Denning, 1998: Interactions between the atmosphere and terrestrial ecosystems: Influence on weather and climate. *Global Change Biol.,* **4,** 461–475.

Pitman, A. J., and M. Zhao, 2000: The relative impact of observed change in land cover and carbon dioxide as simulated by a climate model. *Geophys. Res. Lett.,* **27,** 1267–1270.

Ramankutty, N., and J. A. Foley, 1999: Estimating historical changes in global land cover: Croplands from 1700 to 1992. *Global Biogeochem. Cycles,* **13,** 997–1027.

Rayner, N. A., D. E. Parker, E. B. Horton, C. K. Folland, L. V. Alexander, D. P. Rowell, E. C. Kent, and A. Kaplan, 2003: Global analyses of sea surface temperature, sea ice, and night marine air temperature since the late nineteenth century. *J. Geophys. Res.,* **108,** 4407, doi:10.1029/2002JD002670.

Van den Dool, H. M., and R. M. Chervin, 1986: A comparison of month-to-month persistence of anomalies in a general circulation model and in the earth's atmosphere. *J. Atmos. Sci.,* **43,** 1454–1466.

Vitousek, P. M., H. A. Mooney, J. Lubchenco, and J. M. Melilo, 1997: Human domination of earth's ecosystems. *Science,* **277,** 494–499.

von Storch, H., and F. W. Zwiers, 1999: *Statistical Analysis in Climate Research*. Cambridge University Press, 484 pp.

Wetherald, R. T., R. J. Stouffer, and K. W. Dixon, 2001: Committed warming and its implications for climate change. *Geophys. Res. Lett.,* **28,** 1535–1538.

Winton, M., 2000: A reformulated three-layer sea ice model. *J. Atmos. Oceanic Technol.,* **17,** 525–531.

Xue, Y., M. J. Fennessy, and P. J. Sellers, 1996: Impact of vegetation properties on U.S. summer weather prediction. *J. Geophys. Res.,* **101** (D3), 7419–7430.

Zhao, M., and A. J. Pitman, 2002: The regional scale impact of land cover change simulated with a climate model. *Int. J. Climatol.,* **22,** 271–290.

——, ——, and T. Chase, 2001: The impact of land cover change on the atmospheric circulation. *Climate Dyn.,* **17,** 467–477.

Zwiers, F. W., and H. von Storch, 1995: Taking serial correlation into account in tests of the mean. *J. Climate,* **8,** 336–351.